



## Communication

# A finite element model for investigating the influence of keel design and position on unicompartmental knee replacement cementless tibial component fixation



Alexander MacAulay<sup>\*</sup>, Azmi Rahman, Laurence Marks, David W. Murray, Stephen J. Mellon

Nuffield Department of Orthopaedics, Rheumatology and Musculoskeletal Sciences (NDORMS), Oxford Orthopaedic Engineering Centre (OoEC), University of Oxford, Botnar Research Centre, Oxford, United Kingdom

## ARTICLE INFO

## Keywords:

Oxford unicompartmental knee replacement (OUKR)  
Finite element (FE)  
Interference  
Fixation

## ABSTRACT

**Objectives:** The cementless Oxford Unicompartmental Knee Replacement (OUKR) tibial component relies on an interference fit to achieve initial fixation. The behaviour at the implant-bone interface is not fully understood and hence modelling of implants using Finite Element (FE) software is challenging. With a goal of exploring alternative implant designs with lower fracture risk and adequate fixation, this study aims to investigate whether optimisation of FE model parameters could accurately reproduce experimental results of a pull-out test which assesses fixation.

**Materials and methods:** Finite element models of implants with three methods of fixation (standard keel, small keel, and peg) in a bone analogue foam block were created, in which implants were modelled using an analytical rigid definition and the foam block was modelled as a homogenous linear isotropic material. The total interference and elastic slip were varied in these models and optimised by comparing simulated and experimental results of pull-out tests for two (standard and peg) implant geometries. Then the optimised interference and elastic slip were validated by comparing simulated and experimental data of a third (small keel) implant geometry.

**Results:** The optimisation of parameters established an interference of 0.16 mm and an elastic slip of 0.20 mm as most suitable for modelling the experimental force–displacement plots during pull-out. This combination of parameters accurately reproduced the experimental results of the small keel geometry. The maximum pull-out forces from the FE models were consistent with experimental data for each implant design.

**Conclusions:** This study shows that experimental pull-out tests can be accurately modelled using adjusted interference values and non-linear friction and outlines a method for determining these parameters. This study demonstrates that complex problems in modelling implant behaviour can be addressed with relatively simple models. This can potentially lead to the development of implants with reduced risk of failure.

## Abbreviations

OUKR Oxford Unicompartmental Knee Replacement  
FE Finite Element  
PU Polyurethane

## 1. Introduction

In 2004, the cementless Oxford Unicompartmental Knee Replacement (OUKR, Zimmer Biomet, Swindon, UK) was introduced for the treatment of medial compartment osteoarthritis of the knee. Compared

to the cemented version, the cementless OUKR achieves a lower revision rate and equivalent or better clinical outcomes [1–3]. The cementless OUKR tibial component has similar migration measured by radiostereometric analysis after one year [4,5], and a decreased incidence of tibial radiolucent lines [6,7], suggesting that it has improved fixation. However, there has been concern over the potential of increased risk of tibial plateau fracture, particularly in smaller patients [8]. There is therefore motivation to explore different implant designs to reduce the risk of fracture without compromising fixation.

In the cementless OUKR, initial fixation is achieved through an interference fit, in which the implant is pushed into an undersized cavity

<sup>\*</sup> Corresponding author.

E-mail address: [alexander.macauly@spc.ox.ac.uk](mailto:alexander.macauly@spc.ox.ac.uk) (A. MacAulay).

<https://doi.org/10.1016/j.medengphy.2024.104119>

Received 13 December 2022; Received in revised form 7 November 2023; Accepted 14 February 2024

Available online 15 February 2024

1350-4533/© 2024 The Author(s). Published by Elsevier Ltd on behalf of IPeM. This is an open access article under the CC BY license (<http://creativecommons.org/licenses/by/4.0/>).

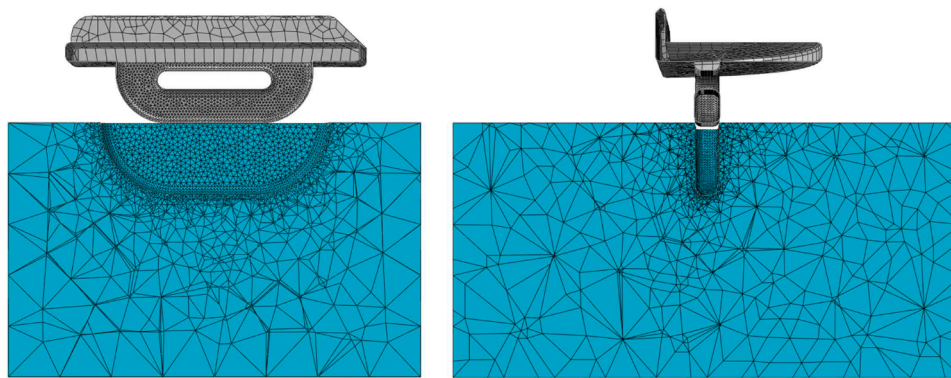


Fig. 1. FE model of the PU foam block and the standard implant.

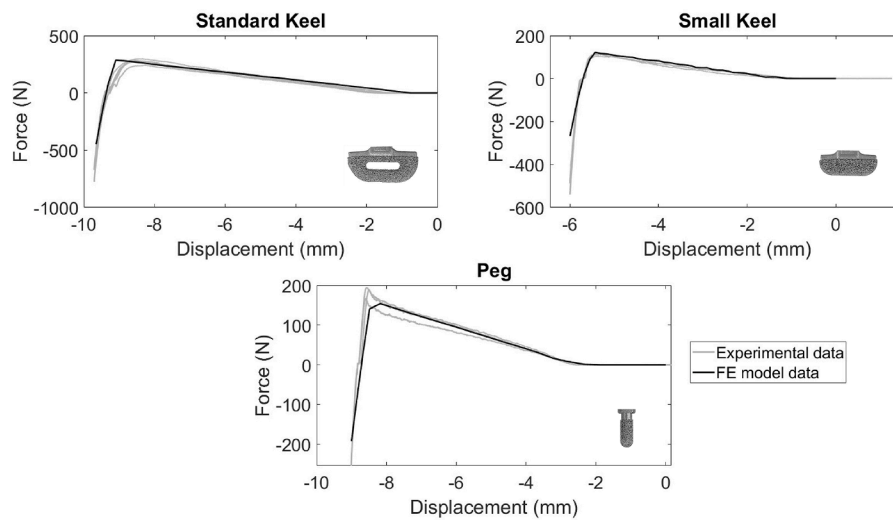


Fig. 2. Pull-out test force–displacement curves for each implant design, comparing experimental and FE model results for an interference of 0.16 mm and an elastic slip of 0.20 mm. More negative displacement values represent depth of implant as it is removed from the foam block.

Table 1

Maximum FE model and experimental pull-out forces for each implant design.

| Implant design | Maximum pull-out force |              |                                 |
|----------------|------------------------|--------------|---------------------------------|
|                | FE                     | Experimental | Experimental standard deviation |
| Standard keel  | 286.1                  | 277.4        | 21.0                            |
| Small keel     | 122.5                  | 113.1        | 6.77                            |
| Peg            | 154.0                  | 184.6        | 14.1                            |

– the difference in size is the interference. The resulting stresses from the interference and friction at the bone-implant interface provide resistance to movement [9]. The current value of interference fit between the implant keel and bone was determined by Campi et al., who concluded that an optimal interference exists which maximises pull-out force while minimising risk of fracture [10].

Previous experimental studies have investigated the effect of interference and implant design on fixation and fracture risk. Rahman et al. found that a smaller keel than is currently used resulted in lower micromotion than the current design, and that interference can counterintuitively increase the micromotion experienced during some movements [11]. Rahman also found that a smaller keel had an increased fracture load compared to the current design, implying a lower risk of fracture [12]. These studies have provided initial evidence that fixation and fracture can be improved through alternative designs.

Finite element (FE) modelling is a useful tool for determining the initial fixation of different designs of cementless components, as it

allows for quantification of the conditions at the bone-implant interface, and parameters can be modified easily to investigate their impact [13]. However, FE models cannot fully reproduce in-vivo conditions and simplifications must be made.

Important parameters when modelling the bone-implant interface include friction coefficient and interference. Previous FE models have used the Coulomb friction model, in which no displacement occurs before maximum friction resistance is reached. In reality, the interface shows large displacements before the maximum shear resistance is reached [14,15]. Models which have implemented this displacement-dependent friction relationship provide better agreement with experimental results than compared to the Coulomb model [16, 17].

In many studies, a linear elastic bone material model is used [16, 18–23]. These material models do not reproduce bone damage. Instead, the interference fit must be adjusted from what is used surgically, as using the same value can cause unrealistic stresses to be generated in the bone [20]. The modelled interference is often chosen to be the value which gives a pull-out force which is close to an experimental reference [16,18,20,21,23]. This method also allows bone damage to be considered in an indirect way; bone is damaged during implant insertion, resulting in a smaller value of interference than the nominal interference. It is important to evaluate whether these models can be used for comparing implant design.

The aim of this study was to optimise the interference and the friction nonlinearity in FE models to reproduce experimental pull-out test

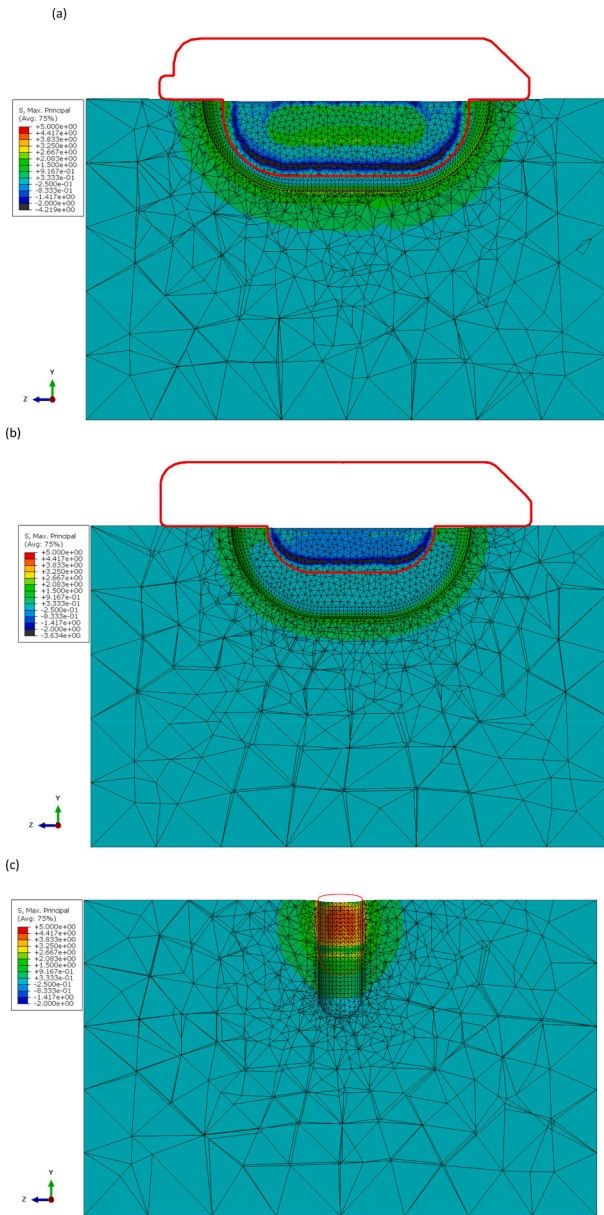


**Fig. 3.** (a)–(c) Maximum principal stresses at full insertion at the surface of the resected slot for the standard keel, small keel, and peg respectively for an interference of 0.16 mm. The positions of the implants are shown as a red outline.

results. FE models and experimental results of pull-out tests of implants from a bone analogue foam block were compared. Two implant geometries were initially calibrated against experimental data to determine the interference and friction to implement in the FE models. These results were then validated by comparing a simulation and experimental data of a third implant geometry.

## 2. Methods

### 2.1. Experimental methodology

Three implant designs were tested experimentally, the currently used keel, a smaller keel, and peg designs. These will be referred to as the standard keel, small keel, and peg respectively (Fig. 1, inset). These implants were implanted in 20 pounds per cube foot (PCF) (Sawbones, Malmö, Sweden) solid polyurethane (PU) foam using a Dartec materials testing machine. These implants were subsequently withdrawn, and the force required to remove them was recorded. The surgically specified interference of 0.8 mm was used. These pull-out tests were repeated three times for the peg and small keel designs, and five times for the standard keel.

### 2.2. Model set-up

An implicit FE model of a polyurethane bone analogue with a density of 20 PCF was developed using ABAQUS (ABAQUS FE, Dassault Systemes, Vélizy-Villacoublay, France). The three implant designs tested experimentally (standard keel, small keel, and peg) were simulated.

The foam was modelled as rectangular blocks ( $L$  65 mm,  $W$  80 mm,  $D$  40 mm) with a centrally positioned slot. The geometry of the slot used experimentally was replicated in the FE model save for the width, which was varied to give different values of interference fit. Values of total interference fit between 0.1 mm and 0.8 mm were simulated.

The foam was meshed using quadratic tetrahedral elements (C3D10), with increased mesh density around the slot. Implants were meshed using triangular elements, with increased mesh density on the keel and the peg tip. Convergence was determined at a mesh size of 1 mm as an increase in mesh density of 60 % resulted in less than 6 % change in maximum pull-out force.

The foam was treated as a homogenous linear elastic isotropic material with Young's modulus of 210 MPa and Poisson's ratio of 0.3 [24]. Implants were modelled using an analytical rigid definition due to the large difference in stiffness between the foam and the implant material [25]. Contact between the foam and the implant was modelled with a surface-to-surface contact definition.

The bone-implant interface was modelled using the Penalty friction formulation in FE modelling software with a coefficient of friction of 0.9, based on previous experimentally measured data. The formulation included options for a shear stress limit and elastic slip allowance,

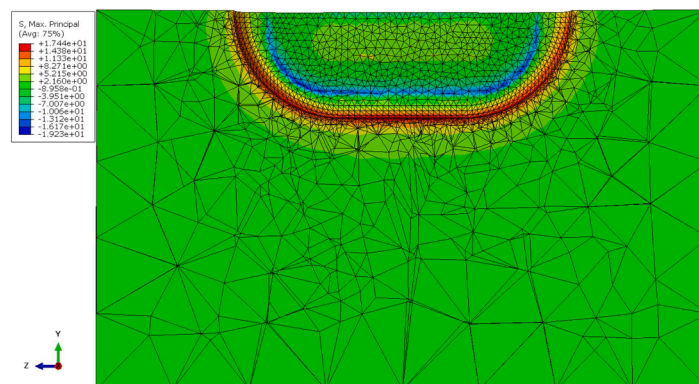


**Fig. 4.** Stress distribution around the standard keel for a modelled interference of 0.8 mm.

reflecting the non-Coulomb friction observed at the bone-implant interface [15].

### 2.3. Boundary conditions and loading

A pull-out test was simulated using displacement control, and the vertical force recorded for each combination of interference and friction coefficient. As the insertion of the implant causes material damage, which was not simulated in this model, only the pull-out segment of the force–displacement plots was used to compare the model to experimental data. The bottom surface of the foam block was defined as encastre, and implant motion was constrained to the y-axis.

### 2.4. Optimisation of model parameters

Initially, 5 values of interference were modelled. It was noted that decreasing interference decreased pull-out force, and increasing the elastic slip increased the displacement at which the peak pull-out force occurred. An iterative method of varying these parameters and comparing the FE solution to the experimental curve was used to find the combination of interference and elastic slip which best reproduced experimental force–displacement plots. This was carried out simultaneously for the peg and standard keel designs to find the combination with the best accuracy across both geometries. This combination was then validated by comparing a simulation and experimental data for the small keel design.

## 3. Results

Fig. 2 shows the results of the parameter optimisation for the three designs. An interference of 0.16 mm and an elastic slip of 0.20 mm was able to reproduce the experimental force–displacement plots during pull-out. This combination over-predicted the maximum pull-out force and gradient of the initial segment of the pull-out test for the standard keel but under-predicted these for the peg design. This combination was chosen as a compromise to minimise these differences and could reproduce experimental data when used in the small keel FE model.

For an interference of 0.16 mm and an elastic slip of 0.20 mm, the maximum pull-out forces from the FE models were consistent with experimental data, as shown in Table 1. Differences in maximum pull-out force between experimental and FE results ranged from 3 % for the standard keel to 17 % for the peg design.

### 3.1. Maximum principal stresses

Fig. 3(a)–(c) show the maximum principal stresses at the surface of the slot for the standard, small, and peg keels respectively for an interference of 0.16 mm. Compressive forces are visible where the implant is in contact with the surface of the foam for both the standard and small keel designs, and there is an increase in maximum principal stress at the bottom of the slot. The stress distribution is different for the peg design, with a tensile stress at the surface of the slot and lower stresses at the bottom of the slot. For all designs, the maximum principal stresses occurred when the implants were fully inserted and decreased as the implant was withdrawn.

Fig. 4 shows the stress distribution for an interference of 0.8 mm, the same as specified surgically. Comparing Figs. 4 to 3(a), which uses an interference of 0.16 mm, the maximum compressive stresses were  $-19.2$  MPa and  $-4.21$  MPa, and the maximum tensile stresses were 17.4 MPa and 4.47 MPa for interferences of 0.8 mm and 0.16 mm respectively. This shows that the interference which is specified surgically is inappropriate to use in linear elastic finite element models, as doing so results in unrealistically large stresses reflecting unmodelled bone damage [24].

## 4. Discussion

This study has shown that it is possible to optimise input parameters to reproduce experimental results which compare different methods of implant fixation in a bone analogue foam.

The results indicate that the optimised combination of interference and elastic slip for two geometries was able to predict the experimental results of a third. This suggests that this combination provides a reasonable approximation of the foam-implant interface. This solution overcomes the challenges faced by linear elastic models in modelling damage at the foam-implant interface, allowing these relatively simple models to be used in future implant modelling such as for implant fixation or fracture risk.

This study has certain limitations. Firstly, as the friction and interference were chosen to replicate experimental results of two different geometries simultaneously, there is a compromise in the accuracy for each individual geometry. However, the motivation for this study is to enable comparisons between designs, and therefore the individual accuracy of the model is less important than the ability to model multiple geometries with reasonable accuracy. In this context, the models were able to return the same rank order of maximum pull-out force as the experiments, indicating that valid comparisons regarding fixation can be made with this model.

Synthetic bone cannot replicate the heterogeneity or damage response of real bone, and the friction coefficients and viscoelasticity differ from those of medial subchondral bone [26,27]. These differences limit the extent to which the findings of this study can be applied to models of real bone. However, this study demonstrates a method for determining FE model parameters which can be used to develop a model of a real tibia in the future. In addition, the goal of these models is to assess alternative designs; complete replication of experimental results is unnecessary provided the model returns similar rankings for the alternative designs.

Further work is required to investigate whether these models can recreate experimental micromotion tests in synthetic bone, as it is this relative motion which determines the long-term fixation of the implant. These models are ultimately aiming to be applied to a model of a real tibia to predict micromotion in-vivo after surgery.

### Ethical approval

None.

### Funding

None.

### Declaration of competing interest

The author or one or more of the authors have received or will receive benefits for personal or professional use from a commercial party related directly or indirectly to the subject of this article. In addition, benefits have been or will be directed to a research fund, foundation, educational institution, or other non-profit organisation with which one or more of the authors are associated. DWM Receives Royalty and Consultancy Payments from Zimmer Biomet Related to Knee Replacement.

### References

- [1] Hooper N, Snell D, Hooper G, Maxwell R, Frampton C. The five-year radiological results of the uncemented Oxford medial compartment knee arthroplasty. *Bone Jt J* 2015;97:1358. <https://doi.org/10.1302/0301-620X.97B10>.
- [2] Pandit H, et al. Improved fixation in cementless unicompartmental knee replacement: Five-year results of a randomized controlled trial. *J. Bone Jt. Surg.* 2013;95:1365–72.

- [3] Mohammad HR, Matharu GS, Judge A, Murray DW. Comparison of the 10-year outcomes of cemented and cementless unicompartmental knee replacements: data from the National Joint Registry for England, Wales, Northern Ireland and the Isle of Man. *Acta Orthop* 2020;91(1):76–81. <https://doi.org/10.1080/17453674.2019.1680924>.
- [4] Kendrick BJL, et al. Histology of the bone-cement interface in retrieved Oxford unicompartmental knee replacements. *Knee* 2012;19(6):918–22. <https://doi.org/10.1016/j.knee.2012.03.010>. Dec.
- [5] Ritter MA, Keating EM, Faris PM, Brugo G. Metal-backed acetabular cups in total hip arthroplasty. *J Bone Jt Surg - Ser A* 1990;72(5):672–7. <https://doi.org/10.2106/00004623-199072050-00005>. Jun.
- [6] Kendrick BJL, et al. Cemented versus cementless Oxford unicompartmental knee arthroplasty using radiostereometric analysis. *Bone Joint J* 2015;97-B(2):185–91. <https://doi.org/10.1302/0301-620X.97B2.34331>. Feb.
- [7] Pandit H, et al. Cementless Oxford unicompartmental knee replacement shows reduced radiolucency at one year. *J Bone Joint Surg Br* 2009;91-B(2):185–9. <https://doi.org/10.1302/0301-620X.91B2.21413>. Feb.
- [8] Hiranaka T, et al. Tibial shape and size predicts the risk of tibial plateau fracture after cementless unicompartmental knee arthroplasty in Japanese patients. *Bone Joint J* 2020;102-B(7):861–7. <https://doi.org/10.1302/0301-620X.102B7.BJ-2019-1754.R1>. Jul.
- [9] Damm NB, Morlock MM, Bishop NE. Friction coefficient and effective interference at the implant-bone interface. *J Biomech* 2015;48(12):3517–21. <https://doi.org/10.1016/j.jbiomech.2015.07.012>. Sep.
- [10] Campi S, et al. Optimal interference of the tibial component of the cementless Oxford unicompartmental knee replacement. *Bone Joint Res* 2018;7(3):226–31. <https://doi.org/10.1302/2046-3758.73.BJR-2017-0193.R1>. Mar.
- [11] Rahman A, Heath D, Mellon S, Murray D. Interference and keel design significantly influence sagittal micromotion in cementless unicompartmental knee arthroplasty. *Orthop Proc* 2023;105-B(SUPP.13):46. <https://doi.org/10.1302/1358-992x.2023.13.046>. –46.
- [12] Rahman A. Assessing and improving clinical outcomes of the cementless Oxford unicompartmental knee replacement tibial component. University of Oxford; 2022.
- [13] Tissakht M, Eskandari H, Ahmed AM. Micromotion analysis of the fixation of total knee tibial component. *Comput Struct* 1995;56(2–3):365–75. [https://doi.org/10.1016/0045-7949\(95\)00029-G](https://doi.org/10.1016/0045-7949(95)00029-G). Jul.
- [14] Rancourt D, Shirazi-Adl A, Drouin G, Paiement G. Friction properties of the interface between porous-surfaced metals and tibial cancellous bone. *J Biomed Mater Res* 1990;24(11):1503–19. <https://doi.org/10.1002/jbm.820241107>. Nov.
- [15] Shirazi-Adl A, Dammak M, Paiement G. Experimental determination of friction characteristics at the trabecular bone/porous-coated metal interface in cementless implants. *J Biomed Mater Res* 1993;27(2):167–75. <https://doi.org/10.1002/jbm.820270205>.
- [16] Dammak M, Shirazi-Adl A, Zukor DJ. Analysis of cementless implants using interface nonlinear friction - Experimental and finite element studies. *J Biomech* 1997;30(2):121–9. [https://doi.org/10.1016/S0021-9290\(96\)00110-8](https://doi.org/10.1016/S0021-9290(96)00110-8). Feb.
- [17] Hashemi A, Shirazi-Adl A. Finite element analysis of tibial implants - effect of fixation design and friction model. *Comput Methods Biomech Biomed Eng* 2000;3(3):183–201. <https://doi.org/10.1080/10255840008915264>.
- [18] Ramamurti BS, Orr TE, Bragdon CR, Lowenstein JD, Jasty M, Harris WH. Factors influencing stability at the interface between a porous surface and cancellous bone: a finite element analysis of a canine in vivo micromotion experiment. *J Biomed Mater Res* 1997;36(2):274–80. [https://doi.org/10.1002/\(SICI\)1097-4636\(199708\)36:2<274::AID-JBM17>3.0.CO;2-G](https://doi.org/10.1002/(SICI)1097-4636(199708)36:2<274::AID-JBM17>3.0.CO;2-G). Aug.
- [19] Viceconti M, Muccini R, Bernakiewicz M, Baleani M, Cristofolini L. Large-sliding contact elements accurately predict levels of bone-implant micromotion relevant to osseointegration. *J Biomech* 2000;33(12):1611–8. [https://doi.org/10.1016/S0021-9290\(00\)00140-8](https://doi.org/10.1016/S0021-9290(00)00140-8). Dec.
- [20] Abdul-Kadir MR, Hansen U, Klabunde R, Lucas D, Amis A. Finite element modelling of primary hip stem stability: the effect of interference fit. *J Biomech* 2008;41(3):587–94. <https://doi.org/10.1016/j.jbiomech.2007.10.009>. Jan.
- [21] Navacchia A, Clary CW, Wilson HL, Behnam YA, Rullkoetter PJ. Validation of model-predicted tibial tray-synthetic bone relative motion in cementless total knee replacement during activities of daily living. *J Biomech* 2018;77:115–23. <https://doi.org/10.1016/j.jbiomech.2018.06.024>. Aug.
- [22] Yang H, et al. Validation and sensitivity of model-predicted proximal tibial displacement and tray micromotion in cementless total knee arthroplasty under physiological loading conditions. *J Mech Behav Biomed Mater* 2020;109:103793. <https://doi.org/10.1016/j.jmbm.2020.103793>. Sep.
- [23] Berahmani S, et al. FE analysis of the effects of simplifications in experimental testing on micromotions of uncemented femoral knee implants. *J Orthop Res* 2016;34(5):812–9. <https://doi.org/10.1002/jor.23074>. May.
- [24] Sawbones. Sawbones solid rigid polyurethane foam 20 pcf density. MatWeb - Mater Prop Data 2022:8–9. 2015. Accessed: Feb. 24[Online]. Available, <http://www.matweb.com/search/datasheet.aspx?MatGUID=d7487588e1504732abe583d6d9252bfa>.
- [25] Pegg EC, et al. Evaluation of factors affecting tibial bone strain after unicompartmental knee replacement. *J Orthop Res* 2013;31(5):821–8. <https://doi.org/10.1002/JOR.22283>. May.
- [26] Grant JA, Bishop NE, Götzen N, Sprecher C, Honl M, Morlock MM. Artificial composite bone as a model of human trabecular bone: the implant-bone interface. *J Biomech* 2007;40(5):1158–64. <https://doi.org/10.1016/j.jbiomech.2006.04.007>. Jan.
- [27] Messer-Hannemann P, Weyer H, Campbell GM, Morlock MM. Time-dependent viscoelastic response of acetabular bone and implant seating during dynamic implantation of press-fit cups. *Med Eng Phys* 2020;81:68–76. <https://doi.org/10.1016/j.medengphy.2020.05.012>. Jul.